

# Nonesterified Fatty Acids Induce Transmembrane Monovalent Cation Flux: Host–Guest Interactions as Determinants of Fatty Acid-Induced Ion Transport<sup>†</sup>

Youchun Zeng,<sup>‡</sup> Xianlin Han,<sup>‡</sup> Paul Schlesinger,<sup>§</sup> and Richard W. Gross<sup>\*,‡</sup>

*Division of Bioorganic Chemistry and Molecular Pharmacology, Departments of Internal Medicine, Chemistry, and Molecular Biology and Pharmacology; Department of Cell Biology and Physiology, Washington University School of Medicine, St. Louis, Missouri 63110*

*Received February 6, 1998; Revised Manuscript Received April 6, 1998*

**ABSTRACT:** Nonesterified fatty acids are key intermediates in cellular metabolism whose intracellular concentration is regulated by multiple anabolic, catabolic, and oxidative enzymatic cascades. Herein, we demonstrate that fatty acids induce transmembrane monovalent cation flux with an apparent rate constant  $k_{app} = 10^{-4} - 10^{-3} \text{ s}^{-1}$ . Fatty acid-induced cation efflux exploits the ionic association of the cation with the carboxylate anion of the fatty acid and the subsequent transmembrane flip-flop of the fatty acid–cation complex. Rates of fatty acid-induced transmembrane cation flux were dependent upon complex host–guest interactions between the fatty acid–cation complex and the phospholipid constituents which comprise the membrane bilayer including (1) the degree of unsaturation of the fatty acid guest and the regiospecificity and stereospecificity of its olefinic linkages; (2) the phospholipid subclass and individual molecular species which constitute the host membrane phospholipids; (3) impedance matching of host and guest hydrophobic characteristics; and (4) the cholesterol content of the membrane bilayer. Arrhenius analysis demonstrated that fatty acid-induced  $\text{K}^+$  efflux was facilitated largely by changes in the entropy of activation of ion translocation and not the energy of activation. Moreover, Arrhenius analysis demonstrated that the energy of activation of ion translocation was phospholipid subclass specific. For example, arachidonic acid-induced cation efflux in membranes comprised of 16:0–18:1 plasmalogen phospholipids possessed an  $E_a = 5.3 \pm 0.4 \text{ kcal/mol}$ , while that for 16:0–18:1 phosphatidylcholine was  $7.2 \pm 0.5 \text{ kcal/mol}$ . Electrophysiologic measurements of planar lipid membranes containing 10 mol % arachidonic acid as a substitutional impurity confirmed the ability of physiologically relevant amounts of fatty acid to induce ion translocation with a specific conductance of  $2.6 \pm 0.3 \mu\text{S/cm}^2$ . Collectively, these results demonstrate that fatty acids facilitate transmembrane cation flux by an ion carrier type mechanism and suggest that fatty acid-mediated ion transport contributes to the leakage current present in many cell types and thus potentially modulates cellular responsivity during signal transduction where the intracellular content of fatty acids changes dramatically.

Mammalian cell membranes are comprised of a diverse array of lipid constituents including phospholipids, nonpolar lipids, and cholesterol which are juxtaposed in a bilayer configuration that provides an effective permeability barrier to the large ionic gradients manifest across cellular membranes. In resting cells, nonesterified fatty acids contribute only a relatively small fraction of total lipid to the membrane lipid pool which has been estimated in most cell membranes to vary from 2 to 5% (1, 2). However, ligand stimulation results in the rapid release of nonesterified fatty acids by the actions of a variety of substrate-specific phospholipases

leading to an abrupt increase in membrane fatty acid concentrations (1–4). Typically, the released fatty acids contain multiple unsaturated centers which are targets for subsequent oxidation and enzyme-mediated covalent transformation resulting in the formation of biologically active eicosanoid metabolites (5, 6). Traditional dogma has emphasized the role of these eicosanoid metabolites as lipid second messengers which mediate their effects after the interaction of each eicosanoid metabolite with its specific receptor counterpart (7, 8). More recently, many direct effects of the released nonesterified fatty acid itself on cellular function have been recognized including its role in modulating (1) ion channel function (9–12), (2) protein kinase C activation (13, 14), and (3) gene transcription (15, 16). It is now well recognized that fatty acid concentrations undergo dramatic increases during cellular activation and that fatty acids themselves are important modulators of cellular function.

Prior studies have demonstrated that the motional regime of nonesterified fatty acids within the membrane bilayer is unique and is distinguished by its rapid transmembrane flip-

<sup>†</sup> This research was supported jointly by grants from the Juvenile Diabetes Foundation International File No. 996003 and NIH Grants 1 PO1 HL 57278-02 and 2 R01 HL 41250-06A1.

\* Author to whom correspondence should be addressed at Washington University School of Medicine, Division of Bioorganic Chemistry and Molecular Pharmacology, 660 South Euclid Avenue, Campus Box 8020, St. Louis, MO 63110. Telephone: 314-362-2690. Fax: 314-362-1402.

<sup>‡</sup> Division of Bioorganic Chemistry and Molecular Pharmacology, Departments of Internal Medicine, Chemistry, and Molecular Biology and Pharmacology.

<sup>§</sup> Department of Cell Biology and Physiology.

flop (rate constants  $k_{\text{ff}} = 10^{-2} - 10 \text{ s}^{-1}$ ) (17–19). Previous work also revealed that fatty acids can exploit their rapid transmembrane flip-flop rates to mediate the transbilayer flux of protons (20). It is largely believed that fatty acid-mediated proton flux leads to the well-known uncoupling effect of fatty acids on mitochondrial oxidative phosphorylation (21, 22). However, to the best of our knowledge, no studies have reported the ability of fatty acids to act as potential (either chemical or electrical) driven transmembrane ion carriers. Herein, we exploit a new technique we have developed that measures the rate of monovalent cation efflux from the intravesicular compartment of small unilamellar vesicles (23) to demonstrate that fatty acids facilitate transmembrane cation flux (e.g.,  $\text{K}^+$  or  $\text{Na}^+$  flux) through an ion carrier mechanism modulated by critical host–guest relationships present in the membrane bilayer. Since the electrophysiologic characterization of transmembrane fatty acid-induced ion translocation demonstrates the likelihood that substantial cellular leakage currents can be attributed to fatty acid-induced cation flux, we propose that fatty acids modulate cellular resting membrane potential and thereby influence a wide variety of potential-dependent cellular responses.

## MATERIALS AND METHODS

**Materials.** Fatty acids and cholesterol were purchased from Nu Chek Prep, Inc. (Elysian, MN). Lysoplasménylcholine (LPlasCho)<sup>1</sup> and plasménylcholine (PlasCho) were synthesized from bovine heart lecithin as described previously (24). Other phospholipids, including lysophosphatidylcholines (LPhosCho) and plasmánylcholines (AlkCho), were purchased from Avanti Polar Lipids, Inc. (Alabaster, AL). All choline glycerophospholipids were further purified by reversed-phase HPLC and extracted twice by the Bligh and Dyer procedure (25). The concentrations of fatty acids and of phospholipids were determined by capillary gas chromatography after acid methanolysis utilizing arachidic acid (20:0) as an internal standard (26). 3, 3'-Dipropylthiadicarbocyanine iodide [ $\text{diSC}_3(5)$ ] was supplied by Molecular Probes, Inc. (Eugene, OR). Most other chemicals were obtained from Sigma Chemical Co. (St. Louis, MO).

**Preparation of Small Unilamellar Vesicles.** Phospholipids or their mixtures with fatty acids and/or cholesterol (2  $\mu\text{mol}$  total lipid) were dissolved in chloroform, dried under a

nitrogen stream, and subsequently subjected to high vacuum (less than 50 mTorr) for at least 2 h. The dried lipid film was suspended in 0.6 mL of medium A (0.29 M  $\text{K}_2\text{SO}_4$  or  $\text{Na}_2\text{SO}_4$ , pH = 6.3) by vigorous vortexing for 2 min and subsequent sonication (4 min, 40% duty cycle) twice utilizing a Vibra Cell Model VC 600 sonicator (Sonics Material, Danbury, CT) under a nitrogen atmosphere. The average diameter of the vesicles, as measured by the light-scattering method (27) with a submicron particle analyzer (Coulter, Hialeah, FL), was about 30 nm, which was consistent with our previous results utilizing inulin trapping (28). The average diameters of vesicles comprised of each choline glycerophospholipid subclass are almost identical within the experimental error. Vesicles containing physiologically relevant ion concentration gradients were prepared with 75 mM  $\text{K}_2\text{SO}_4$  (pH = 6.3) by similar procedures.

**Measurement of Fatty Acid-Induced Membrane Permeability.** In most respects, the procedures were similar to those described previously (23). Typically, sealed vesicles in medium A were diluted 100-fold with a  $\text{K}^+$ -free isoosmotic medium B (e.g., 0.29 M  $\text{Li}_2\text{SO}_4$ , pH = 6.3) to create an ion concentration gradient by addition of 20  $\mu\text{L}$  of vesicles in medium A to 2.0 mL of medium B while stirring. Next, the diluted vesicles were gently stirred for up to 3 days. Passive ion leakage resulted in a change in the ion concentration gradient across the membrane, which was quantified utilizing a potential-sensitive dye [ $\text{diSC}_3(5)$ ] after a valinomycin- or monensin-induced transmembrane potential was generated. After the diluted vesicles had been gently stirred for selected time intervals, 4  $\mu\text{L}$  of  $\text{diSC}_3(5)$  solution (0.27 mg/mL in ethanol) was added with a Hamilton microliter syringe directly to the vesicle solution [final  $\text{diSC}_3(5)$  concentration 1  $\mu\text{M}$ ]. The fluorescence intensities of  $\text{diSC}_3(5)$  were measured with a SLM 4800C spectrofluorometer (SLM Instrument, Urbana, IL) employing an excitation wavelength of 618 nm and an emission wavelength of 690 nm. Ninety seconds after addition of  $\text{diSC}_3(5)$ , 4  $\mu\text{L}$  of valinomycin or monensin solution (final concentration 1  $\mu\text{M}$ ) was injected with the vesicle solution to generate a transmembrane potential. Meanwhile, the fluorescence intensity of  $\text{diSC}_3(5)$  was continuously monitored. The passive ion leakage at each time interval ( $t$ ) can be determined from the magnitude of the residual transmembrane potential created after the addition of valinomycin.

**Measurement of Membrane Conductance Using Planar Lipid Bilayers.** Bilayers were formed by spreading lipids over a 0.25 mm diameter orifice in polystyrene cuvettes and allowing them to thin into a membrane bilayer as described previously (29). Briefly, a lipid solution of 30 mg total lipid in 1 mL of *n*-decane was used to form the bilayer. The lipid composition was varied as indicated. Two microliters of this solution were applied to the cuvette orifice and the solvent was allowed to evaporate. The cuvette was placed in a holder and a solution comprised of 150 mM KCl, 10 mM HEPES (pH = 7.0) was placed on both sides of the orifice. Next, the volume was adjusted so that no hydrostatic pressure differential existed. After 15 min of hydration, a fire-polished glass rod was used to spread lipid from the annulus of the cuvette orifice to form a continuous lipid layer across the opening. Currents were measured under voltage clamp conditions using a Warner 525A bilayer clamp (Warner Instrument Corporation, Hamden, CT) that was connected

<sup>1</sup> ABBREVIATIONS: AlkCho, plasmánylcholine (alkylacyl choline glycerophospholipid);  $\text{diSC}_3(5)$ , 3, 3'-dipropylthiadicarbocyanine iodide; FA, free fatty acid; PlasCho, plasménylcholine; PhosCho, phosphatidylcholine; 14:1-14:1 PhosCho, 1,2-ditetradec-9'-enoyl-*sn*-glycero-3-phosphocholine; 16:0-18:1 PA, 1-hexadecanoyl-2-octadec-9'-enoyl-*sn*-glycero-3-phosphate; 16:0-18:1 PhosCho, 1-hexadecanoyl-2-octadec-9'-enoyl-*sn*-glycero-3-phosphocholine; 16:0-18:1 AlkCho, 1-*O*-hexadecyl-2-octadec-9'-enoyl-*sn*-glycero-3-phosphocholine; 16:0-18:1 Pl-AsCho, 1-*O*-(Z)-hexadec-1'-enyl-2-octadec-9'-enoyl-*sn*-glycero-3-phosphocholine; 16:0-20:4 PhosCho, 1-hexadecanoyl-2-eicosa-5',8',11',14'-tetraenoyl-*sn*-glycero-3-phosphocholine; 16:0-20:4 PlasCho, 1-*O*-(Z)-hexadec-1'-enyl-2-eicosa-5',8',11',14'-tetraenoyl-*sn*-glycero-3-phosphocholine; 20:1-20:1 PhosCho, 1,2-dieicosa-11'-enoyl-*sn*-glycero-3-phosphocholine; 16:0 LPlasCho, 1-*O*-(Z)-hexadec-1'-enyl-2-hydroxy-*sn*-glycero-3-phosphocholine; 18:1 LPA, 1-octadec-9'-enoyl-2-hydroxy-*sn*-glycero-3-phosphate; 18:1 LPhosCho, 1-octadec-9'-enoyl-2-hydroxy-*sn*-glycero-3-phosphocholine; 12:1 FA, 11-dodecenoic acid; 14:1 FA, 9-tetradecenoic acid; 16:1 FA, 9-hexadecenoic acid; 18:1 FA, 9-octadecenoic acid; 20:0 FA, eicosanoic acid (arachidic acid); 20:1 FA, 11-eicosenoic acid; 20:4 FA, 5,8,11,14-eicosatetraenoic acid (arachidonic acid); 22:1 FA, 13-docosenoic acid; 24:1 FA, 15-tetracosenoic acid.

to the bath solution by agar bridges using  $\text{Ag}^+/\text{AgCl}$  electrodes. Data were recorded and analyzed using Axotape (Axon Instruments, Foster City, CA). Total capacitance was monitored with a 100 Hz (10 mV peak-to-peak) triangular voltage signal. Typically, bilayer capacitance measured in this manner was  $\approx 0.4\text{--}0.6 \mu\text{F}/\text{cm}^2$ , with total capacitance being a function of the area of the planar lipid bilayer present in the cuvette orifice. Specific membrane capacitance does not vary markedly with lipid composition (30). The specific membrane capacitance was a function of bilayer thickness, which was held constant by using lipids of constant chain length and dielectric constant of the hydrocarbon side chains ( $\sim 2.1$ ) in these studies. The total membrane capacitance was determined immediately before each voltage step, and the current response was corrected for changes in the area of the membrane bilayer. All determinations were routinely corrected for junction potentials (31).

**Data Analysis.** From the time-course experiments and an experimentally derived calibration curve of fluorescence intensity and transmembrane potential, the concentration of the potassium ions inside the vesicles ( $[\text{K}^+]_{\text{in}}$ ) can be computed as described previously (23). The decrease of  $[\text{K}^+]_{\text{in}}$  with time can be curve-fitted into an exponential equation by using the least-squares method:

$$[\text{K}^+]_{\text{in}} = Ae^{-Bt} + C \quad (1)$$

where  $t$  is time, and  $A$ ,  $B$ , and  $C$  are time-independent constants. The initial rate of the decrease of  $[\text{K}^+]_{\text{in}}$  ( $-d[\text{K}^+]_{\text{in}}/dt$ ) was computed from the first derivatives of the equation at  $t = 0$ . If the initial passive  $\text{K}^+$  efflux is first order with respect to the  $\text{K}^+$  concentration, the apparent rate constant,  $k_{\text{app}}$ , can be calculated from

$$k_{\text{app}} = (-d[\text{K}^+]_{\text{in}}/dt)/[\text{K}^+]_{\text{in}} \quad (2)$$

where  $[\text{K}^+]_{\text{in}}$  is the initial concentration of the potassium ions inside the vesicles (0.58 M). Since the anionic counter currents are negligible with  $\text{SO}_4^{2-}$  buffer, the observed apparent rate constant ( $k_{\text{app}}$ ) of  $\text{K}^+$  efflux reflects the combined rate constant of  $\text{K}^+$  and  $\text{Li}^+$  exchange across the vesicle bilayers. The rate of potassium ion efflux per vesicle can be calculated from the trapped aqueous volume ( $V_{\text{in}}$ ) and the change in the potassium ion concentration inside the vesicle:

$$dN/dt = -6.02 \times 10^{23} V_{\text{in}}(d[\text{K}^+]_{\text{in}}/dt) \quad (3)$$

Assuming the unilamellar vesicles have a diameter of approximately 30 nm and possess a membrane thickness of approximately 4 nm (32), the trapped aqueous volume ( $V_{\text{in}}$ ) is

$$V_{\text{in}} = (4\pi/3)r_{\text{in}}^3 = (4\pi/3)(11^3) \approx 5572 \text{ nm}^3 \quad (4)$$

The whole-vesicle current resulting from  $\text{K}^+$  efflux per vesicle is

$$I = 1.6 \times 10^{-19}(dN/dt) \approx 5.4 \times 10^{-16}(d[\text{K}^+]_{\text{in}}/dt) \quad (5)$$

where  $1.6 \times 10^{-19}$  is the unitary charge of a potassium ion

in coulombs. The current density ( $\sigma$ ) resulting from  $\text{K}^+$  efflux is

$$\sigma = I/(4\pi r^2) \approx 1.9 \times 10^{-19}(d[\text{K}^+]_{\text{in}}/dt) \quad (6)$$

where  $r$  is the average radius of the vesicles (15 nm).

A vesicle having a diameter of 30 nm contains approximately 5500 phospholipid molecules (32). For membranes containing 10 mol % of fatty acid, the number of fatty acid molecules per vesicle is approximately 550. There are two major determinants of the rate of  $\text{K}^+$  efflux: the first is the transmembrane flip-flop of the fatty acid-cation complex; the second is the binding or releasing rate between the fatty acid anions and  $\text{K}^+$  and  $\text{Li}^+$  ions. Assuming one  $\text{K}^+$  ion is transported in each flip-flop cycle (i.e., flip-flop is the rate-controlling step), the effective flip-flop rate of the fatty acid-cation complex molecules is:  $(dN/dt)/550$ .

The apparent activation energy and relative activation entropy of fatty acid-induced  $\text{K}^+$  efflux,  $E_a$  and  $S_a$ , can be calculated by using the following equation:

$$k_{\text{app}} = Ae^{S_a/R}e^{-E_a/RT} \quad \text{or} \quad \ln k_{\text{app}} = \ln A + S_a/R - E_a/RT \quad (7)$$

where  $k_{\text{app}}$  is the apparent rate constant of fatty acid-induced  $\text{K}^+$  efflux,  $R$  is the ideal gas constant ( $8.314 \text{ J mol}^{-1} \text{ K}^{-1}$ ), and  $T$  is the absolute temperature.  $A$  is a probability factor, which was assumed to be identical.

## RESULTS

*Nonesterified Fatty Acids Increase the Passive Ion Permeability of Membrane Vesicles Composed of Plasmalogen Phospholipids.* Vesicles composed of plasmalogen phospholipids [either 16:0–18:1 PlasCho (Figure 1A) or 16:0–20:4 PlasCho (Figure 1E)] did not leak potassium ions even after incubation for 2 h at 22 °C. However, inclusion of only 2% arachidonic acid into the vesicles as a substitutional impurity resulted in the leakage of potassium ions from vesicles composed of 16:0–18:1 PlasCho and the rapid loss of potassium ions from vesicles composed of 16:0–20:4 PlasCho. Increasing the arachidonic acid concentration present in the vesicles to either 5 or 10 mol % resulted in a dose-dependent increase in potassium ion efflux from both plasmalogen phospholipid species (Figure 1).

The temporal dependence of potassium ion efflux from the intravesicular compartment of vesicles composed of 16:0–18:1 PlasCho (Figure 2A) or from 16:0–20:4 PlasCho (Figure 2B) can be calculated from the known internal volume of each vesicle and the experimentally determined fractional loss of potassium ions as described in Materials and Methods. The initial rate constant for potassium ion loss was linear as a function of fatty acid concentration up to 10 mol % (slope for 16:0–18:1 PlasCho  $0.009 \pm 0.001 \text{ min}^{-1}$ , with a correlation coefficient  $r = 0.99$ ; slope for 16:0–20:4 PlasCho  $0.012 \pm 0.001 \text{ min}^{-1}$ , with  $r = 0.99$ ) (Figure 2C). In vesicles composed of 16:0–18:1 PlasCho containing 10 mol % arachidonic acid, the whole vesicle current and the current density were calculated to be  $5.1 \times 10^{-7} \text{ pA}$  and  $17 \text{ nA}/\text{cm}^2$ , respectively, while the current and the current



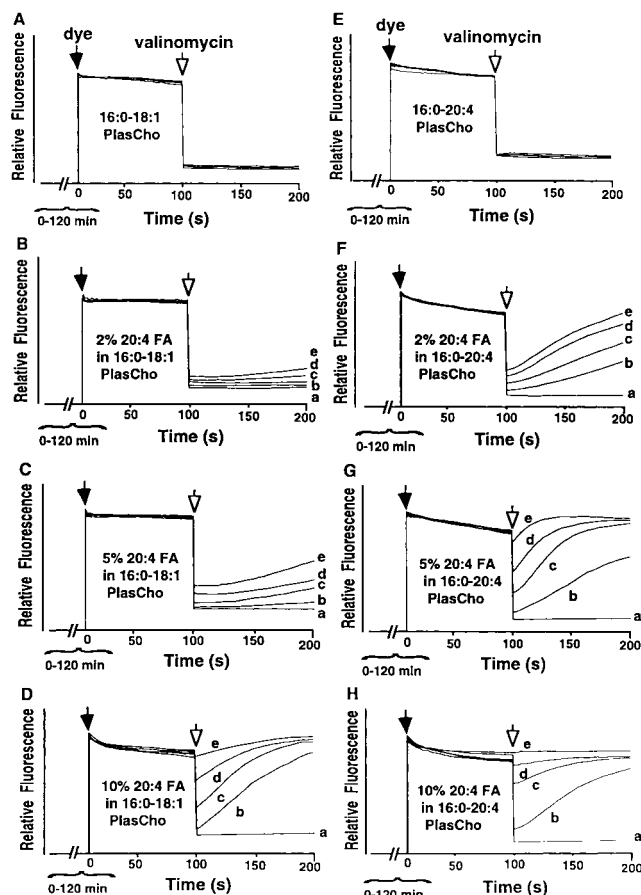


FIGURE 1: Arachidonic acid induces the dose-dependent efflux of potassium ion from vesicles composed of plasmenylcholine. Small unilamellar vesicles ( $d \approx 30$  nm) composed of binary mixtures of 16:0-18:1 PlasCho (left column) or 16:0-20:4 PlasCho (right column) containing the indicated amounts of arachidonic acid were prepared in  $K^+$  medium (0.29 M  $K_2SO_4$ , pH 6.3 at 22 °C) as described in Materials and Methods. Next, vesicles were diluted 100-fold with isoosmotic medium containing  $Li^+$  (0.29 M  $Li_2SO_4$ , pH 6.3 at 22 °C) resulting in the generation of a chemical potential across the bilayers. The diluted vesicles containing the indicated amounts of arachidonic acid were gently stirred for selected time intervals [1 min (b), 30 min (c), 60 min (d), and 120 min (e)] prior to introduction of the potential-sensitive fluorescence dye, diSC<sub>3</sub>-(5) (final concentration,  $1 \times 10^{-6}$  M). The chemical potential at the end of the incubation interval was subsequently transduced into an electrical potential by the addition of valinomycin (final concentration,  $1 \times 10^{-6}$  M), and the resultant changes in fluorescence emission were monitored at 690 nm after excitation at 618 nm utilizing an SLM spectrofluorometer as described in Materials and Methods. In each panel an independent control (a) was performed in which the vesicles were stirred for 120 min in the absence of fatty acid. (▼) and (▽) represent the addition of diSC<sub>3</sub>-(5) and valinomycin, respectively.

density in vesicles comprised of 16:0-20:4 PlasCho containing 10 mol % arachidonic acid were  $6.5 \times 10^{-7}$  pA and 23 nA/cm<sup>2</sup>, respectively. Collectively, these results demonstrate that arachidonic acid induces the rapid release of potassium ions from membrane vesicles composed of plasmenylcholine in a dose-dependent manner which is modulated by the molecular species of plasmenylcholine present in the vesicle bilayer.

**Fatty Acid-Induced  $K^+$  Leakage from Membrane Vesicles Comprised of Different Choline Glycerophospholipid Subclasses.** To determine the dependence of fatty acid-induced potassium ion efflux on the phospholipid subclass present

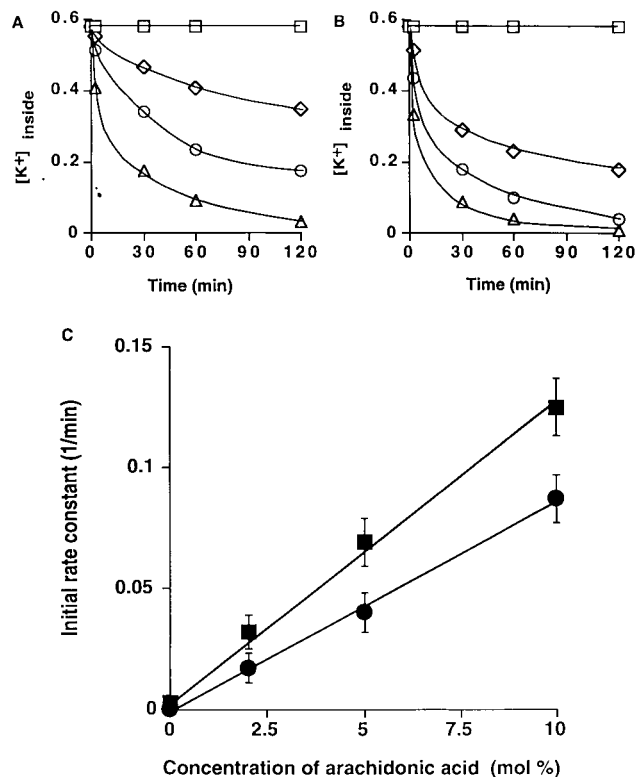


FIGURE 2: Kinetics of arachidonic acid-induced  $K^+$  efflux from phospholipid vesicles. The temporal alterations in fluorescence intensities in Figure 1 were analyzed to determine the kinetics of  $K^+$  loss from the intravesicular compartment. The data from vesicles composed of binary mixtures of either 16:0-18:1 PlasCho (panel A) or 16:0-20:4 PlasCho (panel B) containing 0 mol % ( $\square$ ), 2 mol % ( $\diamond$ ), 5 mol % ( $\circ$ ), or 10 mol % ( $\triangle$ ) of arachidonic acid were analyzed to determine the kinetics of  $K^+$  loss (panels A and B) and the initial rate constants of  $K^+$  efflux across membranes of either 16:0-18:1 PlasCho ( $\bullet$ ) or 16:0-20:4 PlasCho ( $\blacksquare$ ). Rates were calculated from the slope of initial loss of transmembrane chemical potential (Panel C) as described in Materials and Methods. Data shown represent the mean  $\pm$  SD of three independent experiments.

in vesicular membranes, vesicles composed of 16:0-18:1 PlasCho, PhosCho, or AlkCho were prepared in the absence or in the presence of selected amounts of arachidonic acid as described in Materials and Methods. The diameters of vesicles composed of each of these phospholipid subclasses were similar as ascertained by light scattering measurements ( $30 \pm 3$  nm). In the absence of nonesterified arachidonic acid, no potassium ion leakage was manifest over the 2 h incubation period (Figure 3A-C). Moreover, extended incubations of up to 2 days demonstrated that no  $K^+$  leakage could be observed for any subclass (data not shown). In sharp contrast, inclusion of 10 mol % arachidonic acid resulted in the leakage of potassium ions from vesicles composed of each choline glycerophospholipid subclass which was greatest for vesicles composed of plasmenylcholine (PlasCho) and least for vesicles composed of plasmanylcholine (AlkCho). The rate constants of  $K^+$  efflux from vesicles containing 10 mol % arachidonic acid with 90 mol % of 16:0-18:1 PlasCho, 16:0-18:1 PhosCho, or 16:0-18:1 AlkCho were calculated to be 0.09, 0.05, or 0.04 min<sup>-1</sup>, respectively.

To examine the  $K^+/Na^+$  exchange through phospholipid bilayers at physiologic conditions, we prepared vesicles containing physiologically relevant ion gradients with 75 mM

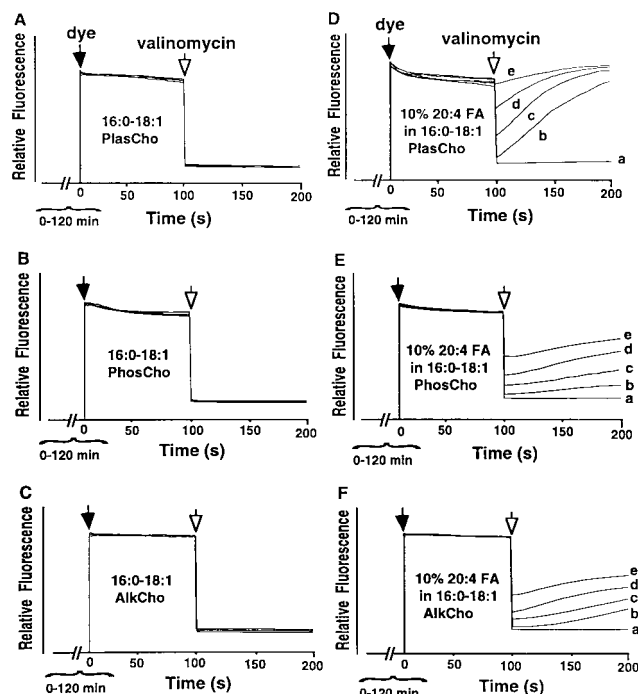


FIGURE 3: Phospholipid subclass-specific alterations in arachidonic acid-induced potassium efflux. Small unilamellar vesicles composed of 16:0–18:1 PlasCho (A), 16:0–18:1 PhosCho (B), 16:0–18:1 AlkCho (C) alone, or the corresponding binary mixtures containing, in addition 10 mol % of arachidonic acid with 16:0–18:1 PlasCho (D), 16:0–18:1 PhosCho (E), 16:0–18:1 AlkCho (F) were prepared in  $K^+$  medium (0.29 M  $K_2SO_4$ , pH 6.3 at 22 °C) and subsequently diluted as described in Materials and Methods. Passive ion permeability was measured as described in the legend to Figure 1 after incubating mixtures for 1 min (b), 30 min (c), 60 min (d), or 120 min (e). In each panel an independent control (a) was performed in which the vesicles were stirred for 120 min in the absence of fatty acid. (▼) and (▽) represent the addition of  $diSC_3(5)$  and valinomycin, respectively.

$K_2SO_4$  on the inside (150 mM  $K^+$ ) and 75 mM  $Na_2SO_4$  and 0.75 mM  $K_2SO_4$  on the outside. In the absence of any fatty acid, no significant ion transport was detected. However, when 10 mol % arachidonic acid was present, an apparent rate constant of monovalent cation efflux  $k = 0.04 \text{ min}^{-1}$  was observed (Figure 4). Thus, at physiologically relevant ionic gradients, fatty acids can induce the transmembrane flux of monovalent cations.

**Dependence of Fatty Acid-Induced Ion Translocation on Ion Characteristics.** To determine the salient structural characteristics of the transported ions, we examined the relative rates of fatty acid-induced ion flux in experiments where either sodium replaced potassium in the intravesicular space, or cesium, sodium or the divalent cation magnesium replaced lithium in the dilution buffer. Experiments utilizing dilution buffer containing sodium (instead of lithium ion) demonstrated that  $K^+$  efflux did not change significantly and thus sodium transport could be supported by fatty acid at similar rates (compare Figure 5, parts A and B). The relative magnitude of sodium transport was investigated by using vesicles loaded with sodium and establishing a sodium concentration gradient prior to the addition of monensin (a sodium selective ionophore) to establish an electrical potential. These experiments demonstrated that sodium and potassium efflux from intravesicular space occurs at similar rates (compare Figure 5, parts A and C). In sharp contrast, utilization of the divalent cation magnesium in the dilution

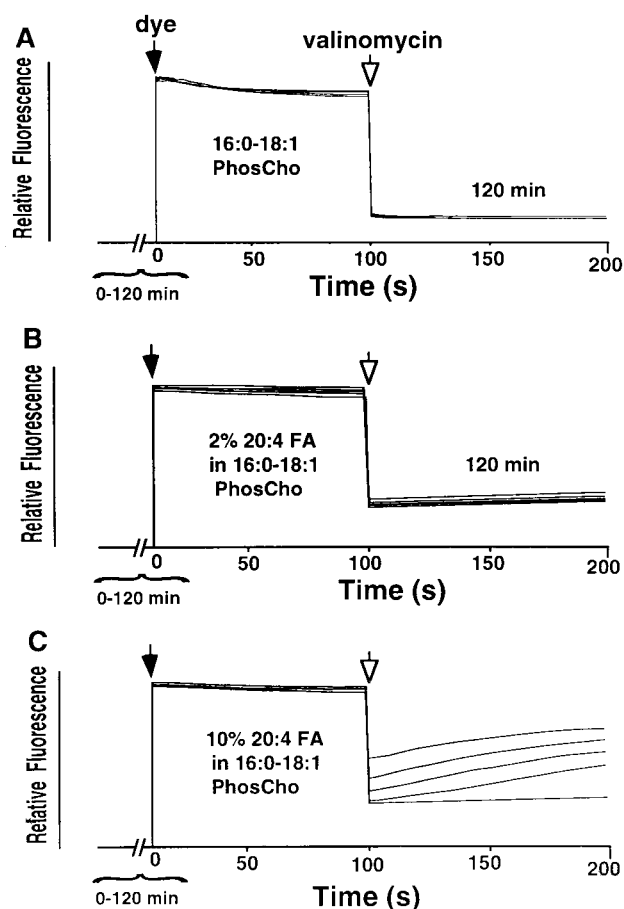


FIGURE 4: Fatty acid-induced  $K^+/Na^+$  exchange across phospholipid bilayers at physiological ion concentration gradients. Small unilamellar vesicles composed of 16:0–18:1 PhosCho alone (A), or the binary mixtures containing 16:0–18:1 PhosCho and in addition, 2 mol % (B) or 10 mol % (C) of arachidonic acid were prepared in  $K^+$  medium (75 mM  $K_2SO_4$ , pH 6.3 at 22 °C) and subsequently diluted with isoionic  $Na^+$  medium (75 mM  $Na_2SO_4$ , pH 6.3 at 22 °C) as described in Materials and Methods. Passive ion permeability was measured as described in the legend to Figure 1 after incubating mixtures for 1 min (b), 30 min (c), 60 min (d), 120 min (e). In each panel an independent control (a) was performed in which the vesicles were stirred for 120 min in the absence of fatty acid. (▼) and (▽) represent the addition of  $diSC_3(5)$  and valinomycin, respectively.

buffer did not support fatty acid-induced efflux of  $K^+$  ion from the intravesicular space (Figure 5D). Collectively, these results demonstrate that fatty acid-induced ion flux does not discriminate between sodium and potassium and that fatty acids cannot support the transport of divalent cations.

**Effect of Fatty Acids on Anion Permeability in Phospholipid Bilayers.** To examine whether fatty acids induce monovalent cation flux by a carrier mechanism or fatty acids induce leakage resulting from destabilization of membrane bilayers, we prepared vesicles containing KCl on the inside and magnesium chloride on the outside in the presence of 0, 10, 20, and 50 mol % fatty acid. No substantial anion leakage was measured in the presence of 0–20 mol % arachidonic acid (Figure 6A–C). In sharp contrast, going from 20 to 50 mol % arachidonic acid resulted in the inability to trap potassium inside the vesicle (Figure 6D). Thus an abrupt change in the membrane properties (vesicle disruption) occurred in going from 20 to 50 mol % fatty acid. Since the hydrated radius of  $K^+$  (2.32 Å) is substantially larger than that of chloride (1.81 Å), these results demonstrate that

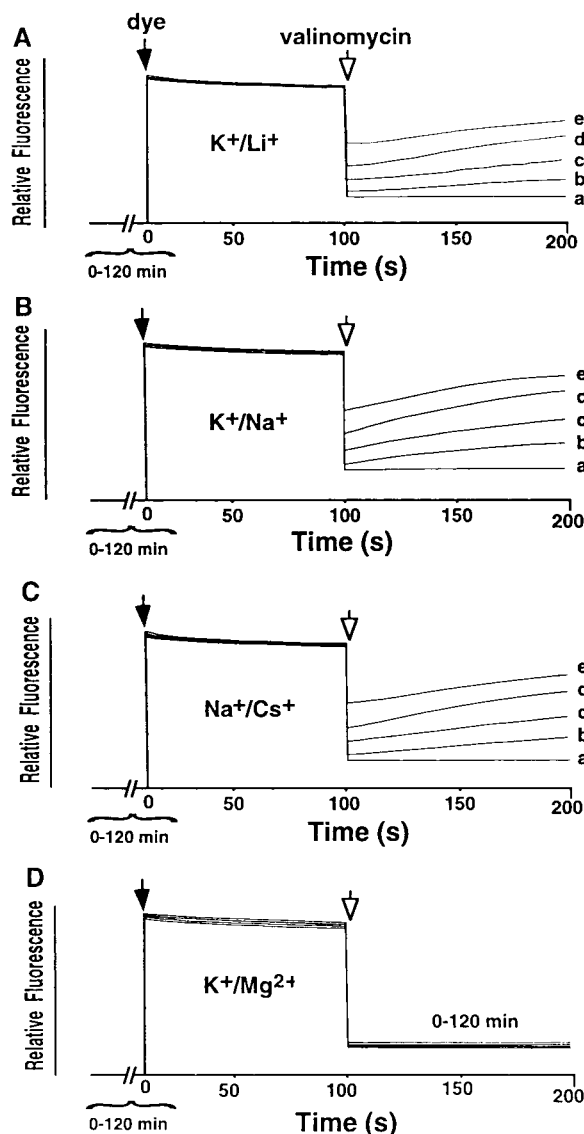


FIGURE 5: Dependence of fatty acid-induced ion translocation on the characteristics of the transported ion. Small unilamellar vesicles composed of 16:0–18:1 PhosCho containing 10 mol % of arachidonic acid were prepared in buffer A [either 0.29 M  $K_2SO_4$  (A, B, or D) or 0.29 M  $Na_2SO_4$  (C), pH 6.3 at 22 °C] and subsequently diluted with isoosmotic buffer B (0.29 M  $Li_2SO_4$  (A),  $Na_2SO_4$  (B),  $Cs_2SO_4$  (C), or  $MgSO_4$  (D), pH 6.3 at 22 °C). Passive ion permeability was measured as described in the legend to Figure 1 after incubating mixtures for 1 min (b), 30 min (c), 60 min (d), and 120 min (e). In each panel an independent control (a) was performed in which the vesicles were stirred for 120 min in the absence of fatty acid. (▼) represents the addition of  $diSC_3(5)$ . (▽) represents the addition of valinomycin (A, B, or D) or monensin (C).

cation flux must necessarily occur by a transport mechanism since intrinsic disruption of the bilayer is insufficient to allow the passage of chloride ions. Collectively, these results support a carrier-mediated mechanism of fatty acid-induced cation transport.

**Structure–Activity Relationships of Lipids in Facilitating  $K^+$  Ion Leakage.** To gain insight into whether the fatty acid-induced leakage of entrapped  $K^+$  ions from phospholipid vesicles was due to changes in membrane fluidity, surface charge, or packing defects or was dependent upon the anionic portion of the hydrophobic constituent, detailed structure–activity studies were performed. First, since lysophospho-

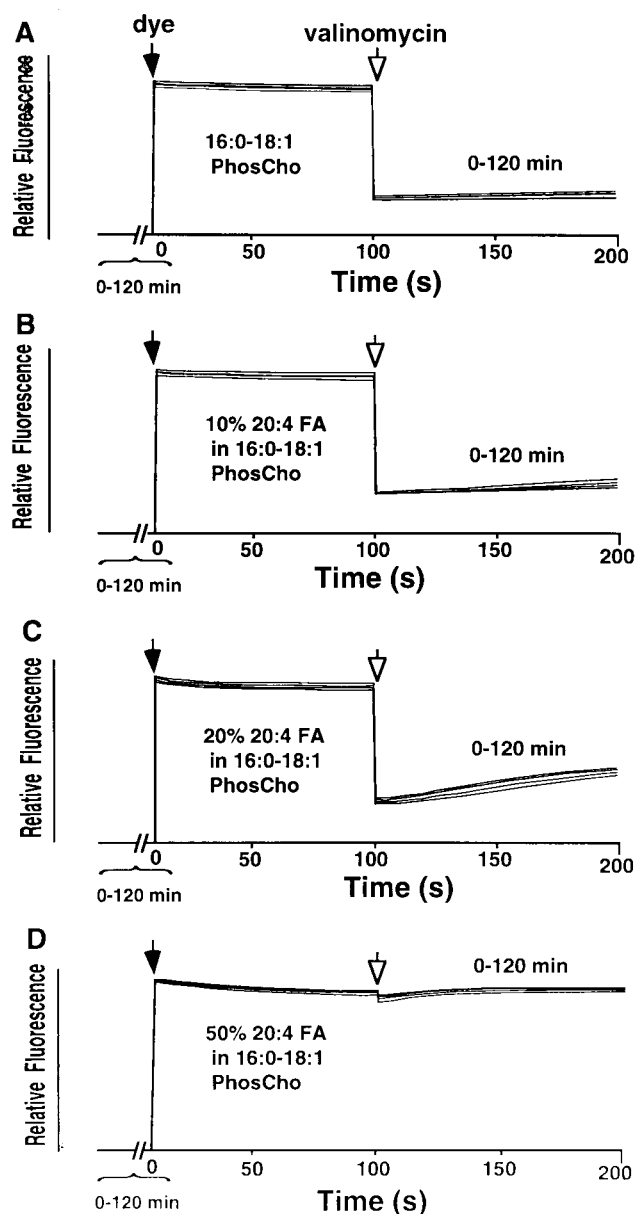


FIGURE 6: Permeability of monovalent anions in bilayers composed of 16:0–18:1 PhosCho. Small unilamellar vesicles composed of 16:0–18:1 PhosCho alone (A), or the binary mixtures containing 16:0–18:1 PhosCho and in addition, 10 mol % (B), 20 mol % (C), and 50 mol % (D) of arachidonic acid were prepared in  $K^+$  medium (0.29 M  $K_2SO_4$ , pH 6.3 at 22 °C) and subsequently diluted as described in Materials and Methods. Passive ion permeability was measured as described in the legend to Figure 1 after incubating mixtures for 1, 30, 60, and 120 min. (▼) and (▽) represent the addition of  $diSC_3(5)$  and valinomycin, respectively.

lipids are both potent perturbers of membrane fluidity and introduce substantial packing defects into membrane bilayers (26, 28, 33), initial experiments examined the effects of various lysophospholipids on potassium ion efflux. Addition of 10 mol % lysophosphatidylcholine (LPhosCho), lysoplasménylcholine (LPlasCho), or lysophosphatidic acid (LPA) did not induce substantial amounts of  $K^+$  ion leakage over the 2 h incubation period (Figure 7B–D). Second, since the negative charge on the fatty acid likely complexes with cations juxtaposed to the membrane bilayer, we examined the effects of the negative charge present in the carboxylate anion on transmembrane ion flux. Removal of the negative charge in fatty acids utilizing either arachidonic acid methyl

ester or arachidonic acid ethyl ester completely ablated fatty acid-induced  $K^+$  ion leakage (Figure 7F,G). Finally, we examined the possibility that increasing negative charge alone could facilitate potassium ion efflux. However, the addition of negative charge alone [e.g., incorporation of LPA, phosphatidic acid (PA), or dicetyl phosphate (data not shown)] also failed to facilitate  $K^+$  ion leakage (Figure 7D,E). Collectively, these results suggest that transmembrane leakage of potassium ions requires both the presence of a negative charge and the ability of the charge-carrying substituent to undergo rapid transmembrane flip-flop (see Discussion).

**Effects of the Fatty Acid Chain Length, Degree of Unsaturation, and Membrane Thickness on the Rate of  $K^+$  Leakage from Phospholipid Vesicles.** To gain further insight into salient features modulating the interaction between fatty acids and their phospholipid hosts, the rate of  $K^+$  efflux utilizing monounsaturated fatty acids with different chain length was examined as a function of phospholipid bilayer thickness. The maximal rate of each monounsaturated fatty acid-induced  $K^+$  leakage was precisely matched to the predicted membrane thickness of each phospholipid host. For example, the maximal rates of  $K^+$  efflux in vesicles composed of 14:1–14:1 PhosCho, 16:0–18:1 PhosCho, or 20:1–20:1 PhosCho were manifest utilizing 16:1 fatty acid, 18:1 fatty acid, or 20:1 fatty acid, respectively (Figure 8). Additional experiments demonstrated that the rate of  $K^+$  efflux increased as a function of the number of double bonds present in the nonesterified fatty acid substitutional impurity (Figure 9). Alterations in the location of the double bond in the fatty acid also substantially affected the rate of  $K^+$  efflux with a rank order 11-octadecenoic acid < 9-octadecenoic acid < 6-octadecenoic acid (Table 1). Finally, a comparison of *cis*- vs *trans*-9-octadecenoic acid demonstrated that the *cis* fatty acid was substantially more potent in inducing  $K^+$  efflux from phospholipid vesicles than its *trans* counterpart (Table 1). Examination of the pH profile of fatty acid-induced  $K^+$  efflux demonstrated that the rates of  $K^+$  efflux increased dramatically from pH 4 to pH 7 and remained constant at pH higher than 7 (Figure 10). Collectively, these results demonstrate that rates of transmembrane flip-flop are highly correlated with the nonesterified fatty acids' ability to induce ion translocation.

**Cholesterol Attenuates Fatty Acid-Induced Ion Efflux from Vesicles Comprised of Plasmalogen or Phosphatidylcholine.** As previously demonstrated, vesicles comprised of either 16:0–18:1 or 16:0–20:4 PlasCho did not leak potassium ions in the absence of fatty acid (Table 2). However, addition of 10 mol % arachidonic acid to vesicles comprised of plasmalogen resulted in over a 100-fold increase in potassium ion efflux which could be attenuated by cholesterol in a dose-dependent fashion (Table 2). Similarly, vesicles comprised of 16:0–18:1 PhosCho did not lose  $K^+$  ion at measurable rates ( $k_{app} < 0.001 \text{ min}^{-1}$ ), but rapidly released potassium ions in the presence of 10 mol % arachidonic acid ( $k_{app} = 0.05 \text{ min}^{-1}$ ). Similar to results with plasmalogen, the addition of cholesterol to vesicles comprised of 16:0–18:1 PhosCho attenuated fatty acid-induced potassium ion efflux (Table 2). Vesicles comprised of 16:0–20:4 PhosCho lost potassium ions at a modest rate ( $k_{app} = 0.04 \text{ min}^{-1}$ ), which was attenuated by the presence of either 15 or 30% cholesterol. The addition of 10 mol % of arachidonic acid to vesicles comprised of 16:0–20:4 PhosCho resulted in a

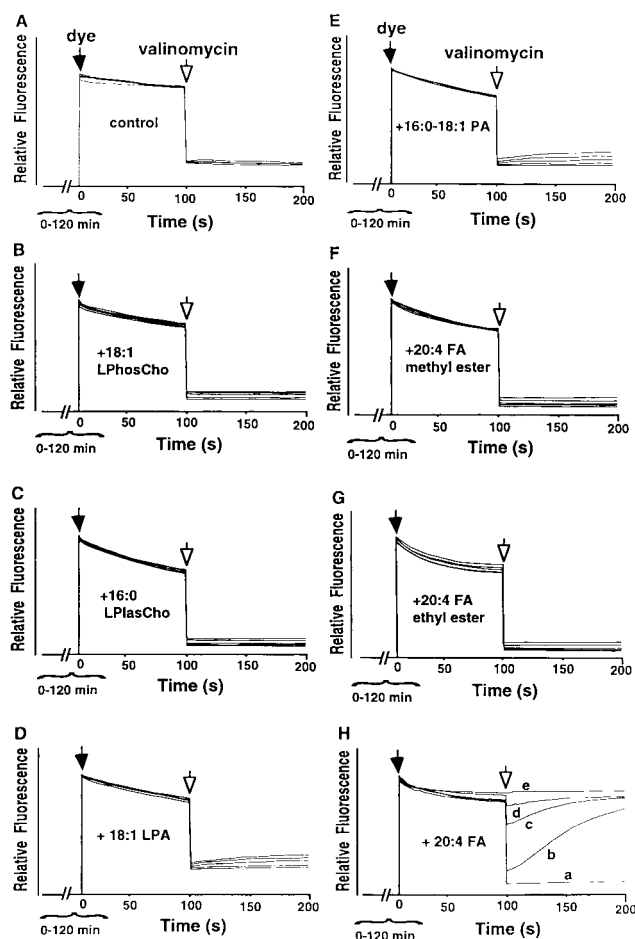


FIGURE 7: Structure-activity relationships of the lipid substitutional impurity on potassium efflux. Small unilamellar vesicles composed of 16:0–20:4 PlasCho (A) alone, or binary mixtures composed of 16:0–20:4 PlasCho with 10 mol % of 18:1 lysophosphatidylcholine (B), 10 mol % 16:0 lysophosphatidylcholine (C), 10 mol % 18:1 lysophosphatidylcholine (D), 10 mol % 16:0–18:1 phosphatidic acid (E), 10 mol % arachidonic acid methyl ester (F), 10 mol % arachidonic acid ethyl ester (G), or 10 mol % free arachidonic acid (H) (control), were prepared in  $K^+$  medium (0.29 M  $K_2SO_4$ , pH 6.3 at 22 °C) and diluted with isoosmotic  $Li^+$  medium to create an ion concentration gradient as described in Materials and Methods. Passive ion permeability was measured as described in the legend to Figure 1 after incubating mixtures for 1 min (b), 30 min (c), 60 min (d), and 120 min (e). In each panel an independent control (a) was performed in which the vesicles were stirred for 120 min in the absence of fatty acid. (▼) and (▽) represent the addition of diSC<sub>3</sub>(5) and valinomycin, respectively.

5-fold increase in  $K^+$  ion permeability which was attenuated, in a dose-dependent fashion, by the inclusion of 15 or 30 mol % cholesterol (Table 2). Collectively, these results demonstrate that cholesterol, presumably by its membrane condensing effect, attenuates fatty acid-induced transmembrane ion flux.

**Determination of the Activation Energies and Relative Entropies of Fatty Acid-Induced Potassium Ion Transport in Vesicles Comprised of Plasmalogen or Phosphatidylcholine by Arrhenius Analysis.** Vesicles composed of 16:0–18:1 PhosCho containing 2, 5, or 10 mol % fatty acid demonstrated a temperature-dependent increase in the apparent rate constant ( $k_{app}$ ) of potassium ion efflux. Comparisons of the vesicles containing 2, 5, or 10 mol % fatty acid demonstrated that the energies of activation for fatty acid-induced  $K^+$  efflux were similar ( $E_a = 7.2 \pm 0.5 \text{ kcal/}$



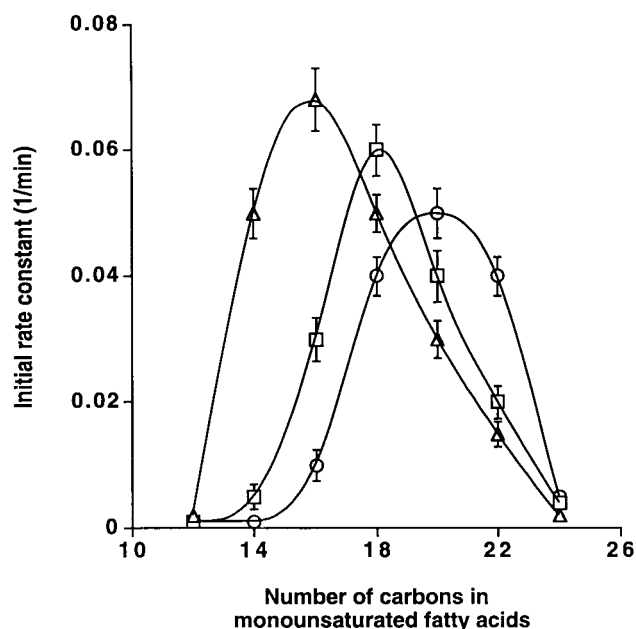


FIGURE 8: The interdependence of fatty acid-induced  $K^+$  efflux on fatty acid chain length and membrane thickness. Small unilamellar vesicles composed of binary mixtures containing 10 mol % of monounsaturated fatty acids with indicated chain lengths (plotted on the  $x$  axis) with 90 mol % of 14:1–14:1 PhosCho ( $\Delta$ ), 16:0–18:1 PhosCho ( $\square$ ), or 20:1–20:1 PhosCho ( $\circ$ ) were prepared in  $K^+$  medium (0.29 M  $K_2SO_4$ , pH 6.3 at 22 °C) and diluted with isoosmotic  $Li^+$  medium to create an ion concentration gradient as described in Materials and Methods. Passive ion permeability was measured as described in the legend to Figure 1. The initial rate constants of  $K^+$  efflux were calculated from the initial slope of loss of transmembrane chemical potential as described in Materials and Methods. Data shown represent the mean  $\pm$  SD of three independent experiments.

mol), and that observed rate differences were due mainly to alterations in the entropies of activation for this process (Figure 11). Similarly, Arrhenius analysis of vesicles composed of 16:0–18:1 PhosCho containing 2, 5, or 10 mol % arachidonic acid demonstrated that the activation energies for each vesicle containing different amounts of arachidonic acid were identical within experimental error ( $E_a = 5.3 \pm 0.4$  kcal/mol). The observed differences in fatty acid-cation transport were mainly dependent upon alterations in the entropies of activation (Figure 11). Collectively, these results demonstrate that increasing mole percentages of arachidonic acid result in enhanced  $K^+$  efflux through changes in the entropy of activation and not the energy of activation (see Discussion).

**Fatty Acid Induces Potassium Flux through Planar Lipid Bilayers under Voltage Clamp Conditions.** To explore the ability of fatty acids to facilitate transmembrane cation transport under conditions where the driving force for ion movement was an imposed electrical potential, we utilized planar lipid membranes containing 0, 2, 5, or 10 mol % arachidonic acid as a substitutional impurity. In planar bilayers composed of phospholipids without incorporated fatty acids, only small amounts of potassium flux occurred during transmembrane holding potentials of  $-80$  to  $+80$  mV. The calculated conductance based upon the slope of the current–voltage relationship was 24 pS (Figure 12). In contrast, at 2, 5, or 10 mol % arachidonic acid present in the planar lipid bilayer, substantial amounts of current were observed which increased with the amount of fatty acid and

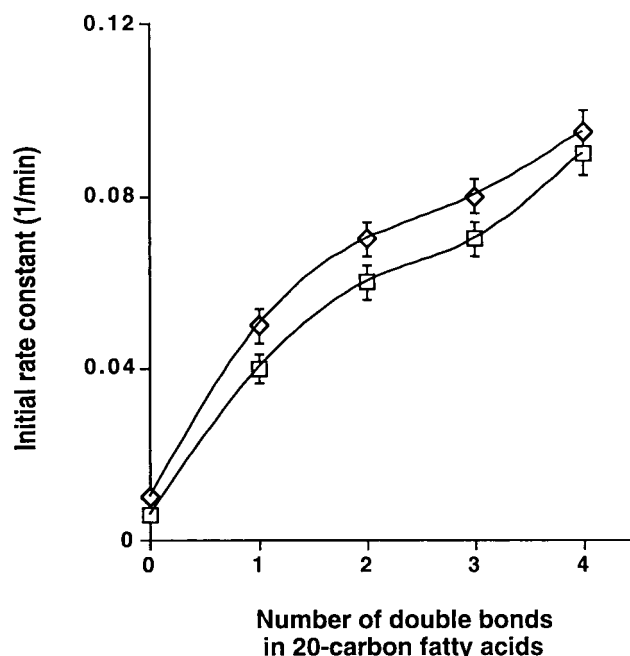


FIGURE 9: The dependence of  $K^+$  efflux across phospholipid bilayers on the number of double bonds present in 20-carbon fatty acids. Small unilamellar vesicles composed of binary mixtures of either 90 mol % 16:0–18:1 PhosCho ( $\square$ ) or 20:1–20:1 PhosCho ( $\diamond$ ) and 10 mol % of the 20-carbon fatty acids [eicosanoic (0), 11-eicosenoic (1), 11,14-eicosadienoic (2), 8,11,14-eicosatrienoic (3), 5,8,11,14-eicosatetraenoic (4)] containing the indicated degrees of unsaturation (plotted on the  $x$  axis), were prepared in  $K^+$  medium (0.29 M  $K_2SO_4$ , pH 6.3 at 22 °C) and diluted into low  $K^+$  medium as described in Materials and Methods. Passive ion permeability was measured as described in the legend to Figure 1. The initial rate constants of  $K^+$  efflux were calculated from the initial slope of loss of transmembrane chemical potential as described in Materials and Methods. Data shown represent the mean  $\pm$  SD of three independent experiments.

Table 1: Effects of Double-Bond Regiospecificity and Stereospecificity in Mono-unsaturated Fatty Acid on the Rate of Fatty Acid-Induced  $K^+$  Efflux

additives	$k_{app}^a$ (1/min)	effective flip-flop rate <sup>b</sup> (1/min)
none	<0.001	<0.004
10% 6-octadecenoic acid	0.07	0.25
10% 9-octadecenoic acid	0.06	0.21
10% 9( <i>trans</i> )-octadecenoic acid	0.04	0.14
10% 11-octadecenoic acid	0.04	0.14

<sup>a</sup> Passive ion flux across bilayers comprised of binary mixtures of 16:0–18:1 PhosCho and 10 mol % of each fatty acid was measured as described in Materials and Methods. The apparent rate constants were calculated from the slope of initial loss of chemical potential, assuming the vesicle had a diameter of 30 nm. <sup>b</sup> The effective flip-flop rates of fatty acids were computed assuming that one potassium ion was transported in each effective flip-flop cycle, as described in Materials and Methods.

the electrical potential applied across the planar lipid bilayer. The calculated conductance for membranes containing 2, 5, or 10 mol % arachidonic acid were  $47 \pm 0.6$ ,  $110 \pm 0.6$ , and  $176 \pm 1.2$  pS, respectively (Figure 12). Collectively, these results demonstrate that arachidonic acid can facilitate electrogenic transmembrane cation flux and that the magnitude of current is related to both the amount of the fatty acid in the membrane bilayer and the driving force predisposing to ion translocation.



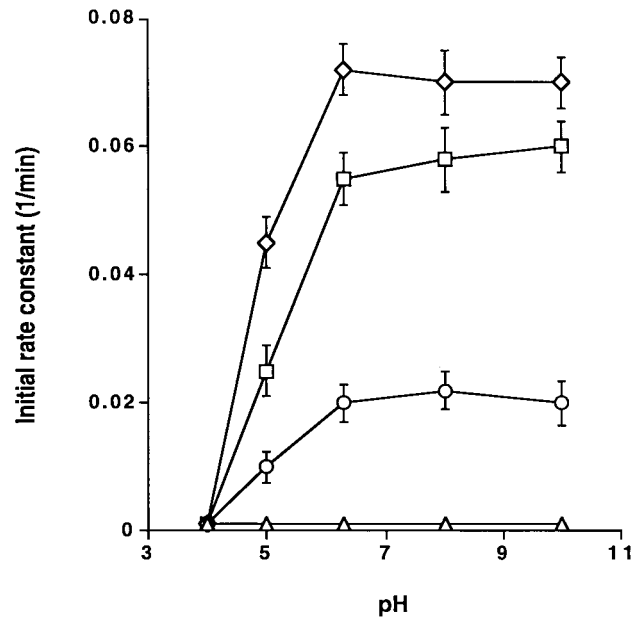


FIGURE 10: pH dependence of fatty acid-induced  $K^+$  efflux across phospholipid vesicles. Small unilamellar vesicles composed of 90 mol % 16:0–18:1 PhosCho containing either 10 mol % 6-octadecenoic acid ( $\diamond$ ), 9-octadecenoic acid ( $\square$ ), 22:1 FA ( $\circ$ ), or 14:1 FA ( $\triangle$ ) were prepared in  $K^+$  medium (0.29 M  $K_2SO_4$ , pH 6.3 at 22 °C) and diluted into low  $K^+$  medium as described in Materials and Methods. Passive ion permeability was measured as described in the legend to Figure 1. The initial rate constants of  $K^+$  efflux were calculated from the initial slope of loss of transmembrane chemical potential as described in Materials and Methods. Data shown represent the mean  $\pm$  SD of three independent experiments.

Table 2: Effects of Cholesterol on Fatty Acid-Induced  $K^+$  Efflux

additives	$k_{app}$ (1/min) <sup>a</sup>			
	16:0–18:1 PhosCho	16:0–20:4 PhosCho	16:0–18:1 PlasCho	16:0–20:4 PlasCho
none	<0.001	0.040	<0.001	<0.002
15% cholesterol	<0.001	0.016	<0.001	<0.001
30% cholesterol	<0.001	0.009	<0.001	<0.001
10% 20:4 FA	0.050	0.22	0.087	0.12
10% 20:4 FA + 15% cholesterol	0.044	0.15	0.072	0.11
10% 20:4 FA + 30% cholesterol	0.040	0.12	0.065	0.10

<sup>a</sup> The rate constants were calculated from the slope of the initial loss of chemical potential, assuming the vesicle has a diameter of 30 nm, as described in Materials and Methods.

# DISCUSSION

The experimental results demonstrate that fatty acids facilitate the efflux of potassium along its concentration gradient with a rate constant in excess of 0.1/min in favorable cases (Figure 2C). Multiple data suggest that the biochemical mechanism responsible for this transport is the association of the monovalent cation to the carboxylate anion of the fatty acid followed by transmembrane flip-flop of a fatty acid-cation complex and subsequent release of the cation as shown in Scheme 1. Specifically, the data demonstrate that alterations in membrane surface charge do not facilitate cation transport if the negatively charged moiety itself cannot undergo rapid transmembrane flip-flop. Moreover, alterations in either membrane dynamics or the introduction of packing defects also do not appear responsible since moieties which are potent perturbants of membrane structure (e.g.,

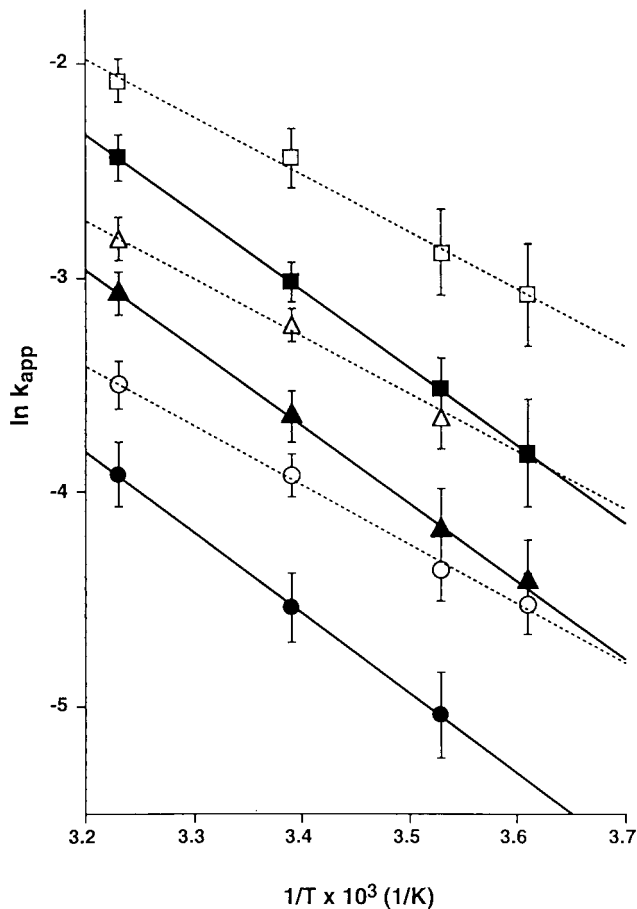


FIGURE 11: Arrhenius plot of fatty acid-induced  $K^+$  efflux across phospholipid bilayers. Small unilamellar vesicles composed of binary mixtures of either 16:0–18:1 PhosCho (open symbol with dashed line) or 16:0–18:1 PlasCho (filled symbol with solid line) containing either 2 mol % ( $\circ$ ), 5 mol % ( $\triangle$ ) or 10 mol % ( $\square$ ) of arachidonic acid were prepared in  $K^+$  medium (0.29 M  $K_2SO_4$ , pH 6.3 at 22 °C) and diluted with isoosmotic  $Li^+$  medium to create an ion concentration gradient as described in Materials and Methods. After incubation at the indicated temperatures for selected time intervals, passive ion permeability was measured as described in the legend to Figure 1. The initial rate constants of  $K^+$  efflux were calculated from the initial slope of loss of transmembrane chemical potential as described in Materials and Methods. Data shown represent the mean  $\pm$  SD of three independent experiments.

lysophospholipids, lysophosphatidic acid, etc.) that markedly alter membrane dynamics and packing do not facilitate cation transport (26, 28, 33). Finally, ablation of the negative charge of the carboxylate anion on the fatty acid by utilization of the cognate methyl or ethyl fatty acid esters does not facilitate cation transport supporting the obligatory role of the carboxylate-cation association proposed in Scheme 1. The case for the proposed model is further strengthened by the demonstration of the importance of specific intramembrane hydrophobic interactions (i.e., host-guest interactions) in modulating the rates of fatty acid-mediated cation transport. For example, alterations in the regiospecificity and stereospecificity of unsaturated centers, alterations in fatty acid chain length in relation to membrane thickness, and alterations in cholesterol content each potentially modulate the rate of fatty acid-facilitated transmembrane cation flux. The inability of fatty acids to induce transbilayer anion flux also strongly supports an ion carrier-mediated transport mechanism. Collectively, the results suggest that fatty acid-

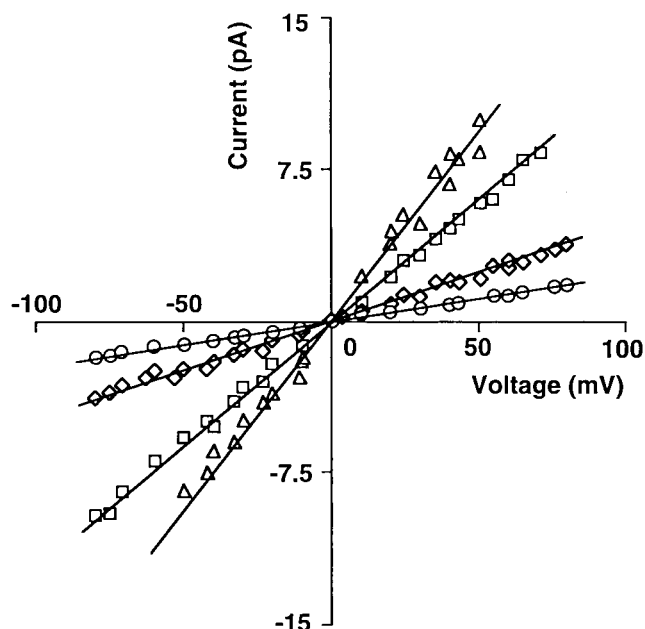
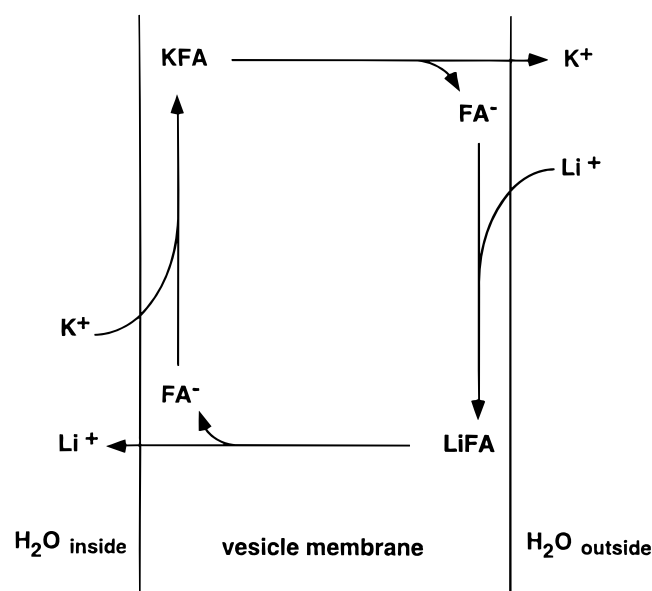


FIGURE 12: Arachidonic acid induces  $K^+$  flux through planar lipid bilayers under voltage clamp conditions. 16:0–20:4 PhosCho alone ( $\circ$ ) or binary mixtures containing 2 mol % ( $\diamond$ ), 5 mol % ( $\square$ ), or 10 mol % ( $\triangle$ ) of arachidonic acid were dissolved in *n*-decane prior to painting over the chamber orifice. After formation of the planar membrane, the current at each indicated holding potential was measured as described in Materials and Methods.

Scheme 1: Proposed Mechanism of  $K^+/Li^+$  Exchange across Phospholipid Bilayers<sup>a</sup>



<sup>a</sup> In the proposed paradigm, fatty acid (FA) binds a  $K^+$  on the inside of the vesicle to form a fatty acid·cation complex (KFA). The KFA complex traverses across the vesicle bilayer to release the  $K^+$  ion. Next, the carboxylate anion on the outside of the vesicle can combine with  $Li^+$  to form a LiFA complex which can flip-flop, resulting in the release of  $Li^+$  ion on the inside of the vesicle. After release, the cycle is complete and the fatty acid is poised for another cycle of ion transport. It should be recognized that not every fatty acid flip-flop needs to be accompanied by an ion. The experimental data represent time averaged rates of only productive cycles or half cycles (i.e., fatty acid flip-flop resulting in ion transport).

facilitated transmembrane cation transport is mediated by the flip-flop of a fatty acid·cation complex.

The rates of transmembrane flip-flop of nonesterified fatty acids are modulated by intricate intermolecular interactions which typify the dynamic chemical associations manifest in host–guest complexes. Prior studies on the modulation of the kinetics of fatty acid transmembrane flip-flop have relied largely on measurements of alterations in intravesicular pH utilizing a pH-sensitive dye, or alternatively, on either fluorescence quenching or fluorescence energy transfer of fluorophores covalently bound to fatty acids (17–20). Utilizing an electrode to measure proton conductance, Gutknecht demonstrated that the rank order of transmembrane flip-flop was oleic > palmitic > myristic > lauric acids in diphytanoyl phosphatidylcholine bilayers (20). Utilizing a fluorescence approach, Kleinfeld et al. demonstrated that transmembrane flip-flop was more rapid in large unilamellar vesicles in comparison to small unilamellar vesicles (17). Apart from these studies, to the best of our knowledge, the molecular details of the types of host–guest interactions which modulate fatty acid transmembrane flip-flop are quite limited. The present results extend the scope of the molecular interactions which modulate transmembrane flip-flop. First, the results demonstrate the importance of specific alterations in the phospholipid subclass and molecular species of the host as important determinants of transmembrane flip-flop rates. Second, the data identify that covalent alterations in the guest including degree of unsaturation as well as the regiospecificity and stereospecificity of the olefin centers are also potent modulators of transmembrane flip-flop rates. For example, increasing the number of double bonds from zero to four results in a 9-fold increase in fatty acid-facilitated cation transport (Figure 9). Similarly, alterations in the location of the double bond ( $\Delta^6$ ,  $\Delta^9$ , or  $\Delta^{11}$ ) also resulted in a 2-fold effect on transmembrane flip-flop rates (Table 1). The presence of a *cis* double bond resulted in a 50% higher rate of fatty acid-facilitated cation flux than the presence of a *trans* double bond. Third, we point out that the precise matching of the effective length of the fatty acid to the membrane thickness is also an important determinant of the rate of fatty acid-facilitated transmembrane cation flux. The waxing and waning of ion transport rates as a function of the chain length of monounsaturated fatty acids in the context of the host underscore the importance of host–guest interactions in this process (Figure 8). In general, all of the results are compatible with the underlying hypothesis that the larger the packing defect in the host–guest complex that the fatty acid engenders, the more rapid transmembrane flip-flop will become (e.g., fatty acid flip-flop increases with the number of double bonds, *cis* > *trans*, proximal > distal olefin linkages). Of similar importance is the necessity to match the length of the fatty acid with the bilayer thickness to minimize the activation energy for the translocation process. We believe this results from the fact that a relatively long fatty acid (relative to its membrane host) must adopt multiple *gauche* linkages to remain within the hydrophobic region of the membrane during the flip-flop process. This would require the presence of even larger membrane packing defects for effective flip-flop than those necessary to accommodate the flip-flop of an all *trans* conformation of the fatty acid. Alternatively, if the fatty acid is too short, significant penetration of the relatively short fatty acid (relative to the thickness of its bilayer host) must occur to facilitate direct

insertion of the carboxylate linkage into the opposite hydrophilic interface.

Study of the dose-response relationships of fatty acid-facilitated ion flux demonstrated that increases in the mole percentage of fatty acid in the membrane resulted in linear increases in fatty acid-induced transmembrane cation flux in membranes composed of either phosphatidylcholine or plasmenylcholine. In each case, Arrhenius analysis demonstrated that fatty acid-induced alterations resulted from a change in the entropy of activation without a change in the energy of activation for fatty acid-facilitated transmembrane cation flux (Figure 11). These results are consistent with the hypothesis that each fatty acid acts independently in the transport process and that the observed activation energy is an intrinsic function of the host-guest relationship between the fatty acid-cation complex and the specific phospholipid molecular constituents which comprise the hydrophobic membrane interior.

Fatty acid-induced transmembrane cation flux was independently verified by the direct electrophysiologic measurement of transmembrane current utilizing a voltage clamp of planar lipid membranes containing incorporated fatty acids as substitutional impurities. Comparisons of the results between the fluorescence measurements and voltage clamp measurements were similar, agreeing within a factor of approximately 10 with each other. The resultant differences are likely due to the modulating effects of membrane curvature on transmembrane fatty acid flip-flop rates. In this regard, Kamp et al. demonstrated 10-fold lower rates of transmembrane flip-flop of fatty acids in small versus large unilamellar vesicles (18).

In planar lipid membranes, a specific conductance of  $2.6 \pm 0.3 \mu\text{S}/\text{cm}^2$  (calculated from the measured conductance and the area of the planar lipid membrane) was found while Gurney et al. demonstrated a specific conductance of  $3 \mu\text{S}/\text{cm}^2$  in myocytes (calculated from Figure 3 of ref 34). In other cell types (e.g., neurons and megakaryocytes), similar values for the specific conductance of the leakage current have been reported (35, 36). Accordingly, from these measurements it would appear that a substantial portion of the leakage current could be attributable to fatty acid-induced ion flux. Since the magnitude of leakage current sets the cells resting membrane potential which represents a critical parameter in mediating cellular physiologic responses, it would follow that alterations in fatty acid content can modulate cellular responsivity through a wide variety of resting membrane potential-dependent mechanisms. In activated cells (e.g., after ligand stimulation or in response to pathophysiologic perturbations such as ischemia) cell membranes can contain from 5 to 15% fatty acid, on the basis of the release of radiolabeled fatty acids from cellular lipids and quantitation by either albumin trapping or quantitative electron microscopic autoradiography (37-40). Thus we believe small amounts of fatty acid-induced ion flux occur in resting cells, and in activated cells larger amounts of fatty acid induced cation flux are manifest as the membrane fatty acid content is increased during physiologic or pathophysiologic perturbations. We specifically point out that fatty acid-modulated ion flux is not solely responsible for the cellular leakage currents (41-45).

In conclusion, the present study demonstrates that non-esterified fatty acids induce cation efflux and that the rates

of this process are dependent upon the properties of the fatty acid (chain length, unsaturation, etc.), properties of the membrane bilayer (thickness, subclass, and molecular species), and the environment in which this process occurs (pH and temperature). In many cell types, ligand stimulation results in an abrupt increase in the concentration of fatty acids in critical subcellular membrane compartments such as the plasma membrane. Accordingly, we propose that the ligand-stimulated phospholipolysis leads to changes in fatty acid-induced cation flux and resultant effects on cellular ion homeostasis and physiologic function.

## REFERENCES

- Boime, I., Smith, E. E., and Hunter, F. E. (1970) *Arch. Biochem. Biophys.* 139, 425-443.
- van der Vusse, G. J., Reneman, R. S., and van Bilsen, M. (1997) *Prostaglandins, Leukotrienes Essent. Fatty Acids* 57, 85-93.
- Madsen, L., Froyland, L., Grav, H. J., and Berge, R. K. (1997) *J. Lipid Res.* 38, 554-563.
- Cooper, R., Noy, N., and Zakim, D. (1987) *Biochemistry* 26, 5890-5896.
- Smith, W. L. (1989) *Biochem. J.* 259, 315-324.
- Janssen-Timmen, U., Tomic, I., Specht, E., Beilecke, U., and Habenicht, A. J. (1994) *Ann. N.Y. Acad. Sci.* 733, 325-334.
- Dennis, E. A. (1987) *Biotechnology* 5, 1294-1300.
- Gross, R. W. (1995) *J. Lipid Mediators Cell Signalling* 12, 131-137.
- Kim, D., and Clapham, D. E. (1989) *Science* 224, 1174-1176.
- Ordway, R. W., Walsh, J. V., and Singer, J. J. (1989) *Science* 224, 1176-1179.
- Gubitosi-Klug, R. A., Yu, S. P., Choi, D. W., and Gross, R. W. (1995) *J. Biol. Chem.* 270, 2885-2888.
- Meves, H. (1994) *Prog. Neurobiol.* 43, 175-186.
- Pajari, A. M., Rasilo, M. L., and Mutanen, M. (1997) *Cancer Lett.* 114 (1-2), 101-103.
- Chen, S. G., and Murakami, K. (1994) *J. Pharm. Sci. Technol.* 48 (2), 71-75.
- Long, S. D., and Pekala, P. H. (1996) *J. Biol. Chem.* 271, 1138-1144.
- Clarke, S. D., and Jump, D. B. (1996) *J. Nutr.* 126, 1105S-1109S.
- Kleinfeld, A. M., Chu, P., and Storch, J. (1997) *Biochemistry* 36, 5702-5711.
- Kamp, F., and Hamilton, J. A. (1992) *Proc. Natl. Acad. Sci. U.S.A.* 89, 11367-11370.
- Kamp, F., Zakim, D., Zhang, F., Noy, N., and Hamilton, J. A. (1995) *Biochemistry* 34, 11928-11937.
- Gutknecht, J. (1988) *J. Membr. Biol.* 106, 83-93.
- Kohnke, D., Ludwig, B., and Kadenbach, B. (1993) *FEBS Lett.* 336, 90-94.
- Schönfeld, P., Schild, L., and Kunz, W. (1989) *Biochim. Biophys. Acta* 997, 266-272.
- Zeng, Y., Han, X., and Gross, R. W. (1998) *Biochemistry* 37, 2346-2355.
- Han, X., Zupan, L. A., Hazen, S. L., and Gross, R. W. (1992) *Anal. Biochem.* 200, 119-124.
- Bligh, E. G., and Dyer, W. J. (1959) *Can. J. Biochem. Physiol.* 37, 911-917.
- Fink, L. W., and Gross, R. W. (1984) *Circ. Res.* 55, 585-594.
- Kolchens, S., Ramaswami, V., Birgenheier, J., Nett, L., and O'Brien, D. F. (1993) *Chem. Phys. Lipids* 65, 1-10.
- Chen, X., Han, X., and Gross, R. W. (1993) *Biochim. Biophys. Acta* 1149, 241-248.
- White, S. H. (1986) in *Ion Channel Reconstitution* (Miller, C., Ed.) pp 3-35, Plenum Press, NY.
- Hille, B. (1992) in *Ionic Channels of Excitable Membranes*, pp 9-12, Sinauer Associates Inc., Sunderland, MA.
- Neher, E. (1995) in *Single Channel Recording* (Sakmann, B., and Neher, E., Eds.) pp 147-153, Plenum Press, New York.

32. Cullis, P. R., and Hope, M. J. (1992) in *Biochemistry of Lipids, Lipoproteins and Membranes* (Vance, D. E., and Vance, J., Eds.) Vol. 20, pp 1–41, Elsevier Science Publishers, Amsterdam, The Netherlands.
33. Han, X., and Gross, R. W. (1991) *Biochim. Biophys. Acta* 1069, 37–45.
34. Osipenko, O. N., Evans, A. M., and Gurney, A. M. (1997) *British J. Pharm.* 120, 1461–1470.
35. Evans, A. M., Osipenko, O. N., and Gurney, A. M. (1996) *J. Physiol.* 496, 407–420.
36. Kapural, L., and Fein, A. (1997) *Biochim. Biophys. Acta* 1326, 319–328.
37. Lehman, J. J., Brown, K. A., Ramanadham, S., Turk, J., and Gross, R. W. (1993) *J. Biol. Chem.* 268, 20713–20716.
38. Saffitz, J. E., Corr, P. B., Lee, B. I., Gross, R. W., Williamson, E. K., and Sobel, B. E. (1984) *Lab. Invest.* 50, 2780–2786.
39. Wolf, M. J., Gross, R. W. (1996) *J. Biol. Chem.* 271, 20989–20992.
40. Wolf, M. J., Wang, J., Turk, J., and Gross, R. W. (1997) *J. Biol. Chem.* 272, 1522–1526.
41. Elinder, F., and Arhem, P. (1991) *NeuroReport* 2, 685–687.
42. Brismar, T., and Collins, V. P. (1989) *Brain Res.* 480, 259–267.
43. Birnir, B., Tierney, M. L., Howitt, S. M., Cox, G. B., and Gage, P. W. (1992) *Proc. R. Soc. London* 250, 307–312.
44. Goldstein, S. A. N., Price, L. A., Rosenthal, D. N., and Pausch, M. H. (1996) *Proc. Natl. Acad. Sci. U.S.A.* 93, 13256–13261.
45. Leonoudakis, D., Gray, A. T., Winegar, B. D., Kindler, C. H., Harada, M., Taylor, D. M., Chavez, R. A., Forsayeth, J. R., and Yost, C. S. (1998) *J. Neurosci.* 18, 868–877.

BI980303U